

## Hydrogen peroxide and nitric oxide induce anticontractile effect of perivascular adipose tissue via renin angiotensin system activation



Natália Nóbrega<sup>a</sup>, Natália Ferreira Araújo<sup>a</sup>, Daniela Reis<sup>a</sup>, Larissa Moreira Facine<sup>a</sup>, Claudiane Aparecida S. Miranda<sup>a</sup>, Gianne Campos Mota<sup>b</sup>, Rosária Dias Aires<sup>c</sup>, Luciano dos Santos Aggum Capettini<sup>b</sup>, Jader dos Santos Cruz<sup>c</sup>, Daniella Bonaventura<sup>a,\*</sup>

<sup>a</sup> Laboratory of Vascular Pharmacology, Department of Pharmacology, Institute of Biological Science, Federal University of Minas Gerais, Brazil

<sup>b</sup> Laboratory of Vascular Biology, Department of Pharmacology, Institute of Biological Science, Federal University of Minas Gerais, Brazil

<sup>c</sup> Laboratory of Excitatory Membranes, Department of Biochemistry and Immunology, Institute of Biological Science, Federal University of Minas Gerais, Brazil

### ARTICLE INFO

#### Keywords:

Perivascular adipose tissue  
Renin-angiotensin system  
Angiotensin 1-7  
Mice aorta  
Nitric oxide and hydrogen peroxide

### ABSTRACT

The perivascular adipose tissue (PVAT) is located around the adventitia, composed primarily by adipocytes, stromal cells, leukocytes, fibroblasts and capillaries. It is well described that PVAT is an important modulator of the vascular tone being considered a biologically active tissue, releasing both vasoconstrictor and vasodilator factors. The literature shows that the anti-contractile effect induced by PVAT may be due to activation of the renin-angiotensin system (RAS).

**Aim:** Investigate whether the renin-angiotensin system participates in the effect exerted by perivascular adipose tissue on the vascular tone.

**Methods and results:** For this study we used thoracic aorta from Balb/c mice and performed vascular reactivity, nitric oxide and hydrogen peroxide quantification using selective probes and fluorescence microscopy, immunofluorescence to locate receptors and enzymes involved in this response. Our results demonstrated that perivascular adipose tissue induces an anti-contractile effect in endothelium-independent manner and involves Mas and AT<sub>2</sub> receptors participation with subsequent PI3K/Akt pathway activation. This pathway culminated with nitric oxide and hydrogen peroxide production by neuronal nitric oxide synthase, being hydrogen peroxide most relevant for the anti-contractile effect of perivascular adipose tissue.

**Conclusion:** For the first time in the literature, our results show the presence of Mas and AT<sub>2</sub> receptors, as well as, nitric oxide synthase on perivascular adipose tissue. Furthermore, our results show the involvement of Mas and AT<sub>2</sub> receptors and consequently nitric oxide synthase activation in the anti-contractile effect exerted by perivascular adipose tissue.

### 1. Introduction

The perivascular adipose tissue (PVAT) is characterized as a supporting tissue or lipid storage and a dynamic endocrine organ capable for secreting growth factors that influence smooth muscle cell

proliferation [1], adipokines and cytokines that regulate inflammatory processes [2], as well as, vasoconstrictor and vasodilator factors that participate in the control of the vascular tone, in a paracrine manner [3,4]. Based in these characteristics, it is possible to affirm that various adipose tissue, such as PVAT, are structures with important functions,

**Abbreviations:** ACh, Acetylcholine; ACE, Angiotensin Converting Enzyme; ACE II, Angiotensin-Converting Enzyme type II; Akt, Protein Kinase B; Ang II, Angiotensin II; Ang 1–7, Angiotensin 1–7; AT<sub>2</sub>, Ang II receptor type II; BAT, Brown Adipose Tissue; BSA, Bovine Serum Albumin; CaCl<sub>2</sub>, Calcium Chloride; CO<sub>2</sub>, Carbon Dioxide; DAF – FMDA, 4-amino-5-methylamino-2',7'-difluorescein diacetate; DAPI, 4',6-diamidino-2-phenylindole dihydrochloride; EC<sub>50</sub>, Concentration inducing response corresponding to 50% of maximum effect; Emax, Maximal Effect; eNOS, Endothelium Nitric Oxide Synthase; H2DCF-DA, 2',7' dichlorodihydrofluorescein diacetate; H<sub>2</sub>O<sub>2</sub>, Hydrogen Peroxide; KCl, Potassium Chloride; KH<sub>2</sub>PO<sub>4</sub>, Anhydrous Monobasic Potassium Phosphate; L-NAME, Nω-Nitro-L-arginine methyl ester hydrochloride; L-NNA, L-NG-nitroarginine; Mas, Ang 1–7 receptor; MgSO<sub>4</sub>, Magnesium sulfate; Mn, Milinewton; NaCl, Sodium Chloride; NaHCO<sub>3</sub>, Sodium Bicarbonate; NO, Nitric Oxide; NOS, Nitric Oxide Synthase; nNOS, Neuronal Nitric Oxide Synthase; O<sub>2</sub>, Oxygen; PBS, Phosphate Buffered Saline; pD<sub>2</sub>, Potency (-log EC<sub>50</sub>); pH, Hydrogen Potential; Phe, Phenylephrine; PI3K, Phosphatidylinositol 3-kinase; PVAT, Perivascular Adipose Tissue; RAS, Renin Angiotensin System; SEM, Standard Error Mean; WAT, White Adipose Tissue; 7-Ni, 7-Nitroindazole

\* Corresponding author. Department of Pharmacology, Institute of Biological Sciences, Av. Antonio Carlos, 6627, 31270-100 Belo Horizonte, MG, Brazil.

E-mail address: [danibona@gmail.com](mailto:danibona@gmail.com) (D. Bonaventura).

<https://doi.org/10.1016/j.niox.2018.12.011>

Received 8 October 2018; Received in revised form 23 November 2018; Accepted 31 December 2018

Available online 03 January 2019

1089-8603/ © 2019 Elsevier Inc. All rights reserved.

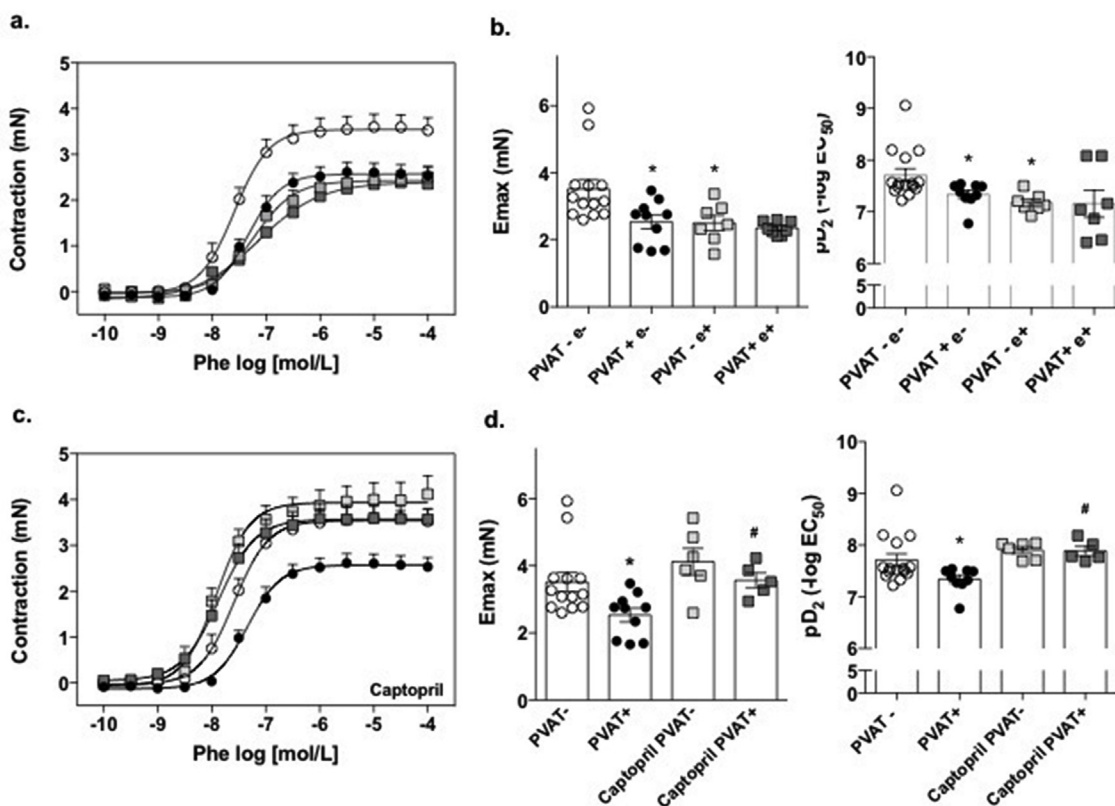


**Fig. 1.** Evaluation of the effect of PVAT and the involvement of ACE derivatives in the contraction induced by Phe in aortic rings. a-c: Cumulative concentration-response curves for Phenylephrine were performed in intact or denuded (e+/-) aortic rings with and without PVAT (PVAT+/-) (a) and curves for Phenylephrine performed in denuded aortic rings in the presence of Captopril (c). b-d. Bars with distribution of the data represent the mean ± SEM of values of Emax and pD<sub>2</sub> of the contraction induced by Phe obtained in independent preparations. Emax and pD<sub>2</sub> values in denuded or intact aortas, with or without PVAT, and denuded aortas incubated with Captopril. (PVAT+ e+: n = 8; PVAT- e+: n = 7; PVAT+ e-: n = 10; PVAT- e-: n = 13; Captopril PVAT-: n = 6; Captopril PVAT+ n = 5) \*Represents a significant difference (\*p < 0.05 when compared to PVAT- e-).

**Table 1**  
**Emax and pD<sub>2</sub> values in aortas endothelium denuded, with and without PVAT, incubated or not.** \*\*Represents a significant difference (\*p < 0.05 when compared to PVAT- e-; #p < 0,05 when compared to PVAT+ e-).

Groups	Emax (mN)	pD <sub>2</sub> (-log EC <sub>50</sub> )
Control PVAT- e+	2.50 ± 0.22 (n = 7)*	7.17 ± 0.07 (n = 7)*
Control PVAT+ e+	2.35 ± 0.07 (n = 8)	7.15 ± 0.22 (n = 8)
Control PVAT- e-	3.52 ± 0.28 (n = 13)	7.62 ± 0.08 (n = 13)
Control PVAT+ e-	2.53 ± 0.20 (n = 10)*	7.32 ± 0.07 (n = 10)*
PVAT- Captopril	4.12 ± 0.40 (n = 6)	7.90 ± 0.07 (n = 6)
PVAT+ Captopril	3.57 ± 0.22 (n = 5)#	7.88 ± 0.09 (n = 5)#
PVAT- A779	4.19 ± 0.33 (n = 5)	7.96 ± 0.12 (n = 5)*
PVAT+ A779	3.56 ± 0.19 (n = 6)#	7.76 ± 0.06 (n = 6)#
PVAT- PD123,319	3.73 ± 0.17 (n = 5)	8.00 ± 0.1 (n = 5)*
PVAT+ PD123,319	2.29 ± 0.22 (n = 6)	7.81 ± 0.07 (n = 6)#
PVAT- LY-294,002	3.77 ± 0.28 (n = 5)	8.0 ± 0.11 (n = 5)*
PVAT+ LY-294,002	3.84 ± 0.5 (n = 5)#	7.81 ± 0.09 (n = 5)#
PVAT- L-NAME	4.91 ± 0.34 (n = 5)*	7.65 ± 0.04 (n = 5)
PVAT+ L-NAME	4.49 ± 0.41 (n = 6)#	7.64 ± 0.06 (n = 6)#
PVAT- L-NNA	4.73 ± 0.35 (n = 5)*	8.30 ± 0.08 (n = 5)*
PVAT+ L-NNA	3.81 ± 0.26 (n = 7)#	8.19 ± 0.16 (n = 7)*
PVAT- 7-Ni	3.85 ± 0.27 (n = 6)	7.35 ± 0.21 (n = 6)*
PVAT+ 7-Ni	3.51 ± 0.38 (n = 6)#	7.07 ± 0.17 (n = 6)#
PVAT- Catalase	4.02 ± 0.37 (n = 5)	7.99 ± 0.12 (n = 5)
PVAT+ Catalase	3.56 ± 0.22 (n = 5)#	7.88 ± 0.08 (n = 5)#
PVAT- Carboxy-PTIO	5.47 ± 0.56 (n = 7)*	8.29 ± 0.04 (n = 7)*
PVAT+ Carboxy-PTIO	5.51 ± 0.19 (n = 5)#	8.12 ± 0.08 (n = 5)#

endocrine and paracrine, regulated by complex mechanisms [5–7].

PVAT is composed by adipocytes that surround blood vessels, with its composition varying between white adipose tissue (WAT) and brown adipose tissue (BAT), whereas the amount of the BAT and WAT in the

PVAT varies according to the location of the blood vessel [8]. Moreover, the PVAT is characterized as a very moldable tissue since the profile factors released by it varies depending on location and situation in which it is subject. In some situations, the PVAT present a vasodilator profile, releasing for example, perivascular relaxation factor (PVRF) [9–11], adiponectin [12], leptin [13], angiotensin 1-7 (Ang 1-7) [14], hydrogen peroxide (H<sub>2</sub>O<sub>2</sub>) [4] and nitric oxide (NO) [15]. Furthermore, PVAT can present a vasoconstrictor profile, can be releasing angiotensin II (Ang II) [16] and superoxide anions [17].

Among the various mediators released by PVAT described in the literature, Ang 1-7, an important component of the renin-angiotensin system (RAS), has been described that influences the control of the vascular tone [14]. Additionally, in 2011 researchers groups showed that the relaxation response exerted by PVAT in rat aorta is dependent on Mas receptors activation, another component of RAS [14,18]. Furthermore, it has been shown that the activation of Mas receptors induces the activation of nitric oxide synthase (NOS) leading to the synthesis of a potent vasodilator, nitric oxide (NO), through the PI3k-Akt activation [19]. Knowing that in rat aorta the PVAT could release Ang 1-7, as vasodilator factor, and the relaxation response induced by this peptide involves the activation of Mas receptors, leading a NOS activation producing a potent vasodilators, such as NO, the aim of this present study is to verify if the RAS participates in the effect triggered by PVAT on the control of vascular tone in mice aorta, as well as, to identify where receptors and enzymes are locate.

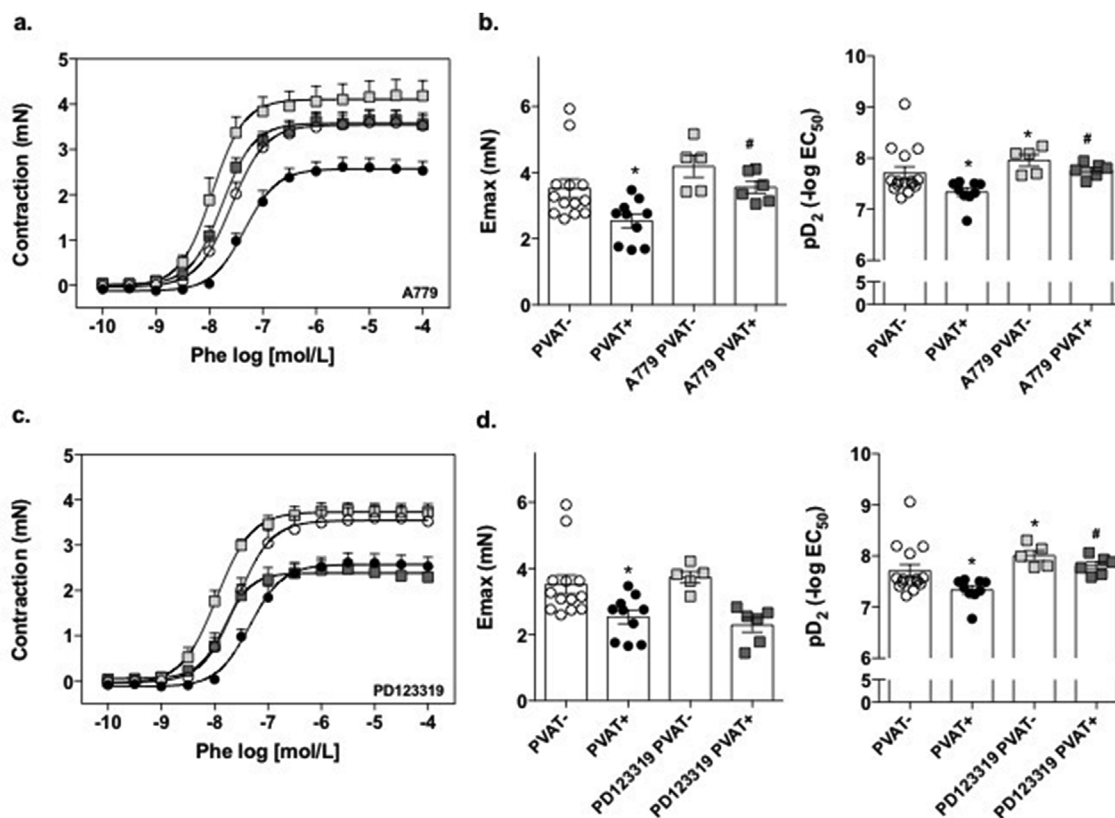


**Fig. 2.** Evaluation of Mas and AT<sub>2</sub> receptors involvement on effect of PVAT. **a-c.** Cumulative concentration-response curves for Phenylephrine, incubated with A779 or PD123319 respectively, were performed in denuded aortic rings with and without PVAT. **b-d.** Bars with distribution of the data represent the mean  $\pm$  SEM of values of Emax and pD<sub>2</sub> of the contraction induced by Phe, in aortic rings incubated with A779 or PD123319, obtained in independent preparations. Emax and pD<sub>2</sub> values in denuded aortas, with or without PVAT, and aortas incubated with A779 or PD123319. (A779 PVAT-: n = 5; A779 PVAT+ n = 6; PD123319 PVAT-: n = 5; PD123319 PVAT+ : n = 6). \*\*Represents a significant difference (\*p < 0.05 when compared to PVAT-; #p < 0,05 when compared to PVAT+).

## 2. Methods

### 2.1. Animals

Male Balb/c mice 8–12 week old (25–30 g) were used, maintained under controlled conditions of light-dark cycle and temperature (24–26 °C) with free access to rodents chow and water. Mice were euthanized by decapitation and all procedures were carried out in accordance with the guidelines from Directive 2010/63/EU of the European Parliament on the protection of animals and was approved and reviewed by the Animal Ethics Committee of Federal University of Minas Gerais (n° 225/2013).

### 2.2. Vessel preparation and isometric tension measurement

The thoracic aorta was quickly removed and cut into 2–3 mm length rings. To evaluate the participation of PVAT and endothelium in vascular responses, both were removed in some rings. The aortic rings were placed between two stainless-steel stirrups and connected to an isometric force transducer (World Precision Instruments, Inc., Sarasota, FL, USA). The rings were placed in an organ chamber containing Krebs solution with the following composition (mmol/L): 135.0 NaCl, 5.0 KCl, 1.17 KH<sub>2</sub>PO<sub>4</sub>, 1.4 MgSO<sub>4</sub>, 20.0 NaHCO<sub>3</sub>, 11.0 glucose, and 2.5 CaCl<sub>2</sub>. The solution was maintained at pH 7.4 gassed with 95% O<sub>2</sub> and 5% CO<sub>2</sub> at 37 °C. The rings were initially stretched to a basal tension of 4.9 mN, and then they were allowed to equilibrate for 60 min. Endothelial integrity was assessed by relaxation induced by ACh (10<sup>-6</sup> mol/L) in the presence of contractile tone induced by phenylephrine (Phe 10<sup>-7</sup> mol/L). For studies of endothelium-denuded vessels, the rings were discarded if there was any degree of relaxation. Furthermore, mechanical

removal of the endothelium did not lead to damage of the vascular smooth muscle cells, since the maximal response induced by phenylephrine was greater than that observed in intact mice aorta as expected [20].

### 2.3. Experimental protocols

#### 2.3.1. Concentration-effect curves for phenylephrine (Phe)

To evaluate the vascular contraction induced by a receptor activation, cumulative concentration-effect curves for Phe (10<sup>-10</sup> mol/L - 10<sup>-4</sup> mol/L) were performed in aortic rings with and without endothelium, in the presence or absence of PVAT.

After this protocol, all the others protocols were performed in aortic rings without endothelium, in the presence or absence of PVAT.

#### 2.3.2. Renin angiotensin system involvement

Cumulative concentration-effect curves for Phe (10<sup>-10</sup> mol/L - 10<sup>-4</sup> mol/L) were performed after pre-incubated for 30 min with Captopril (10<sup>-5</sup> mol/L) to evaluate the involvement of ACE (Angiotensin Converting Enzyme) derivatives in PVAT response. To evaluate the role of Mas and AT<sub>2</sub> receptors in the vascular response induced by PVAT, aortic rings were pre-incubated for 30 min with Mas and AT<sub>2</sub> antagonist, A779 (10<sup>-6</sup> mol/L) and PD123,319 (10<sup>-6</sup> mol/L), respectively [21–23].

#### 2.3.3. Implication of PI3k-Akt-NOS pathway activation

Cumulative concentration-effect curves for Phe (10<sup>-10</sup> mol/L - 10<sup>-4</sup> mol/L) were performed after pre-incubation (30 min) with Ly-294,002 (10<sup>-6</sup> mol/L), a selective PI3k inhibitor. Knowing that PI3k-Akt pathway can activate NOS, stimulating NO production, cumulative

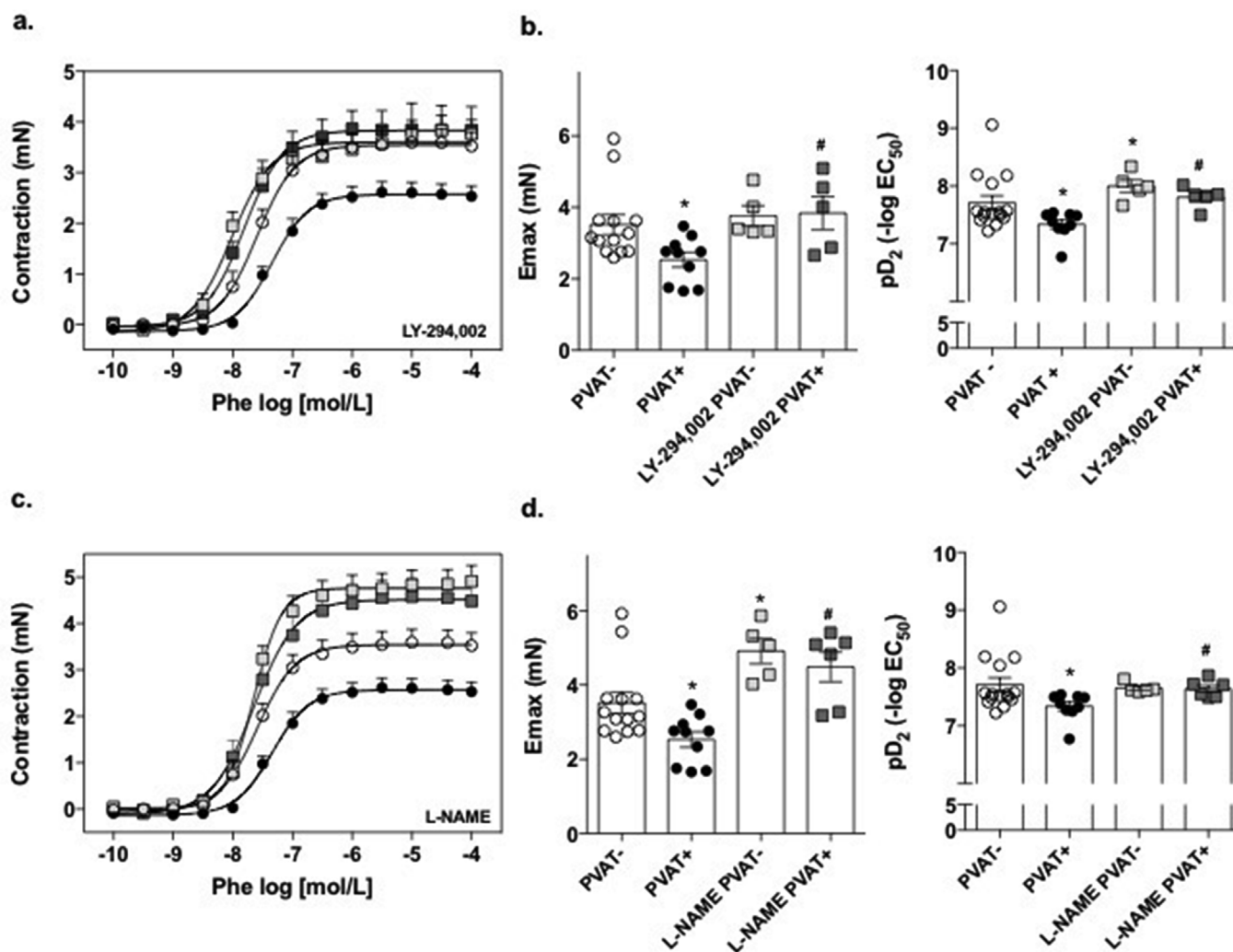


**Fig. 3.** Evaluation of the PI3K-Akt pathway and NOS activation involvement on the effect of PVAT. **a-c.** Cumulative concentration-response curves for Phenylephrine, incubated with LY294002 or L-NAME, were performed in denuded aortic rings with and without PVAT. **b-d.** Bars with distribution of the data represent the mean ± SEM of values of Emax and pD<sub>2</sub> of the contraction induced by Phe, in aortic rings incubated with LY294002 or L-NAME, obtained in independent preparations. Emax and pD<sub>2</sub> values in denuded aortas, with or without PVAT, and aortas incubated with LY-294.002 or L-NAME. (LY-294.002 PVAT-: n = 5; LY-294.002 PVAT+ n = 5; L-NAME PVAT-: n = 5; L-NAME PVAT+: n = 6). \*#Represents a significant difference (\*p < 0.05 when compared to PVAT+; #p < 0,05 when compared to PVAT+).

concentration-effect curves for Phe (10<sup>-10</sup> mol/L - 10<sup>-4</sup> mol/L) were performed in the presence of a non selective NOS inhibitor (L-NAME - 10<sup>-4</sup> mol/L), or selective nNOS inhibitor (7-Ni - 10<sup>-4</sup> mol/L) or selective eNOS inhibitor (L-NNA 10<sup>-6</sup> mol/L) [24,25].

**2.3.4. NO and H<sub>2</sub>O<sub>2</sub> involvement**

To verify if NO and H<sub>2</sub>O<sub>2</sub> are involved in PVAT effect on vascular tone, cumulative concentration-effect curves for Phe (10<sup>-10</sup> mol/L - 10<sup>-4</sup> mol/L) were performed after pre-incubated with carboxy-PTIO (10<sup>-4</sup> mol/L) and catalase (300 U/mL-30 min) respectively [26–28].

**2.4. NO and H<sub>2</sub>O<sub>2</sub> detection**

Fluorescent probes 4-amino-5-methylamino-2',7'-difluorescein diacetate (DAF-2DA; code: D23842; Invitrogen, USA) and 2',7'-dichlorodihydrofluorescein diacetate (H<sub>2</sub>DCF-DA; code: D399; Invitrogen, USA) were used to evaluate NO and H<sub>2</sub>O<sub>2</sub> production, respectively, in mice aorta [29,30]. Briefly, the aortic rings in the presence or absence of perivascular adipose tissue were incubated with 10 μmol/L of DAF or DCF at 37 °C. After 30 min, the rings were washed in Krebs–Henseleit solution for 10 min embedded in Tissue-Tek®

O.C.T.™ freezing medium (Sakura®, USA) and frozen at -20 °C for obtaining cryosections. The vessels were cut and mounted in slides and digital images were obtained through fluorescence microscope (Zeiss) using the 40× objective. The images were analyzes using the ImageJ 1.46 software by measuring the mean optical density of the fluorescence. Ten fields per slide of media layer and perivascular tissue were measured. The mean of fluorescence from each slide was plotted and analyzed using GraphPad Prism 6 (GraphPad Software Corporation, version 6, 2010, La Jolla, CA, USA) [30,31].

**2.5. Fluorescence microscopy**

Frozen thoracic aortas were removed and serially cut in 10 μm transversal sections. Sections were fixed in cold 100% acetone for 20 min, and then washed with phosphate buffer (PBS) 1 × for 3 times. The fixed cryosections of the thoracic aorta were rinsed in wash buffer (4% BSA + 0.1% Triton X-100, in PBS). Following appropriate blocking procedures (3% BSA in PBS; 30 min), slides were incubated with rabbit monoclonal anti-Mas (code: AAR-013; 1:100; Alomone Labs) or mouse anti-nNOS (code: sc-5302; 1:100; Santa Cruz Biotechnology); mouse anti-eNOS (code: sc-136977; 1:100; Santa Cruz Biotechnology); rabbit

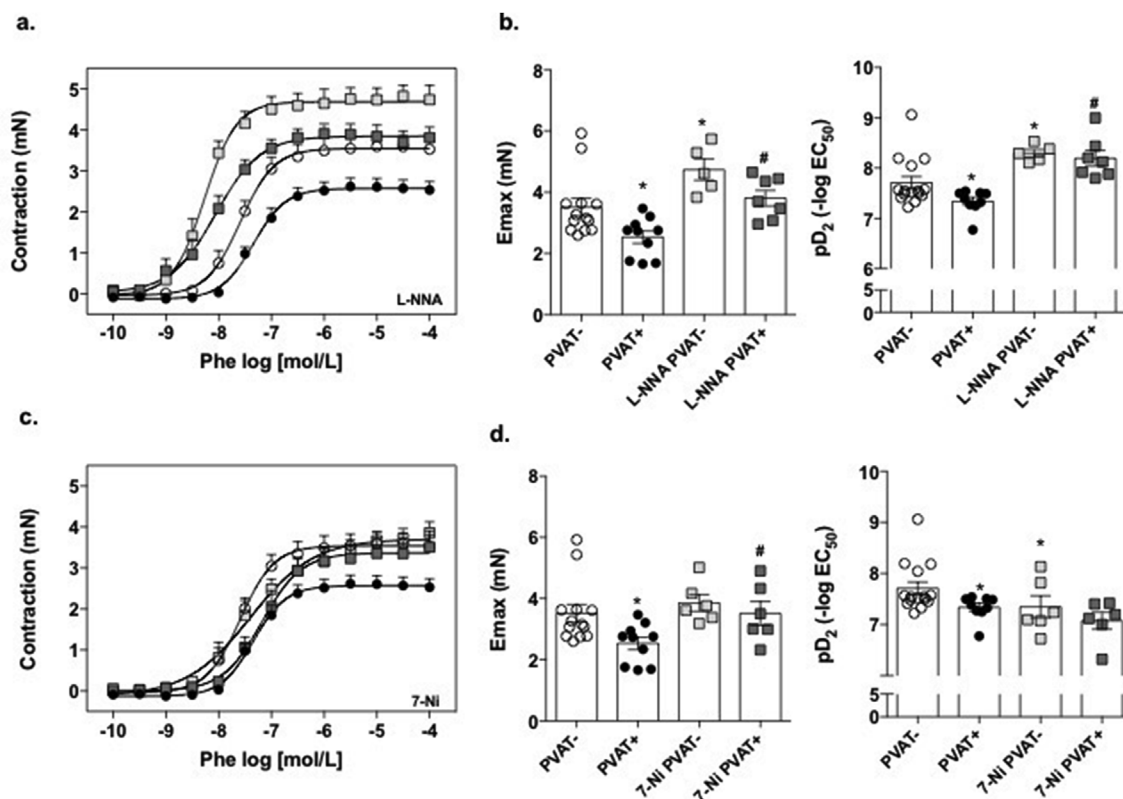


**Fig. 4.** Evaluation of the involvement of eNOS and nNOS on the effect of PVAT in vascular contraction induced by Phe. a-c. Cumulative concentration-response curves for Phenylephrine, incubated with L-NNA/7-Ni respectively, were performed in denuded aortic rings with and without PVAT. b-d Bars with distribution of the data represent the mean  $\pm$  SEM of values of Emax and  $pD_2$  of the contraction induced by Phe, in aortic rings incubated with L-NNA/7-Ni respectively, obtained in independent preparations. Emax and  $pD_2$  values in denuded aortas, with or without PVAT, and aortas incubated with L-NNA or 7-Ni. (L-NNA PVAT-: n = 5; L-NNA PVAT+ n = 7; 7-Ni PVAT-: n = 6; 7-Ni PVAT+: n = 6). \*#Represents a significant difference (\*p < 0.05 when compared to PVAT-; #p < 0.05 when compared to PVAT+).

anti-AT<sub>2</sub> (code: AAR-012; 1:100; Alomone Labs); overnight at 4 °C followed by incubation with goat anti-mouse secondary antibody conjugated with Alexa Fluor 488 (code: sc-362257; 1:200; Santa Cruz Biotechnology) and goat anti-rabbit secondary antibody conjugated with Alexa Fluor 594 (code: A-11037; 1:200; Invitrogen) for 2 h. The sections were examined with a Nikon Eclipse Ti microscope (Nikon, USA) with excitation at 488/594 nm and emission at 520/600 nm. The fluorescence (arbitrariness) intensity was measured using ImageJ<sup>®</sup> software 1.42q (Wayne Rasband, NIH). Seven fields per slide of perivascular tissue were measured. The mean of fluorescence from each slide was plotted and analyzed using GraphPad Prism 6 (GraphPad Software Corporation, version 6, 2010, La Jolla, CA, USA). Fluorescence intensity in mouse aorta was expressed as fold increase [32].

## 2.6. Drugs and reagents

In this study we used acetylcholine (ACh), phenylephrine (Phe), Captopril, A779, PD123,319, LY-294,002, NG-nitro-L-arginine (L-NAME), L-NG-nitroarginine (L-NNA), 7-nitroindazol (7-NI), carboxy-PTIO, catalase, DAF-2DA and H<sub>2</sub>DCF-DA that were obtained from Sigma-Aldrich and Invitrogen respectively (USA). All solutions of drugs were prepared as follows in deionized water, except catalase that was prepared in physiology solution 0.9%. DAF-2DA and H<sub>2</sub>DCF-DA was prepared in dimethylsulphoxide (DMSO) which concentration did not exceed 0.5%. For immunofluorescence we used rabbit monoclonal anti-Mas (code: AAR-013; 1:100; Alomone Labs) or mouse anti-nNOS (code: sc-5302; 1:100; Santa Cruz Biotechnology); mouse anti-eNOS (code: sc-136977; 1:100; Santa Cruz Biotechnology); rabbit anti-AT<sub>2</sub> (code: AAR-012; 1:100; Alomone Labs); goat anti-mouse secondary antibody

conjugated with Alexa Fluor 488 (code: sc-362257; 1:200; Santa Cruz Biotechnology) and goat anti-rabbit secondary antibody conjugated with Alexa Fluor 594 (code: A-11037; 1:200; Invitrogen).

## 2.7. Data and statistical analysis

Data and statistical analysis comply with the recommendations on experimental design and analysis in pharmacology [33]. Graphs and analyzes of the vascular reactivity experiments were performed on the GraphPad Prism 6 program (GraphPad Software Corporation, version 6, 2010, La Jolla, CA, USA). Squares nonlinear regression method (Meddings et al., 1989) were used for determinations of EC<sub>50</sub>. The concentration of the agents that produced the half maximal contraction amplitude, which was determined after log transformation of the normalized concentration–response curves and it is reported as negative logarithm ( $pD_2$ ), and maximal effect (Emax) was considered as the maximal amplitude response reached in the concentration–effect curves for the contractile agent. Contractile response induced by Phe was analyzed using one-way ANOVA with post-hoc test Holm-Sidak with significance set at p < 0.05. Data were expressed as means  $\pm$  SEM.

## 3. Results

### 3.1. Cumulative concentration-response curves for phenylephrine (Phe) in denuded or intact aorta in the presence or absence of PVAT

As shown in Fig. 1a and b, in aortas with endothelium, the presence or absence of PVAT did not show any significant difference on vascular contraction induced by Phe. However, in the absence of endothelium, the maximum contraction (Emax) and potency ( $pD_2$ ) for Phe was

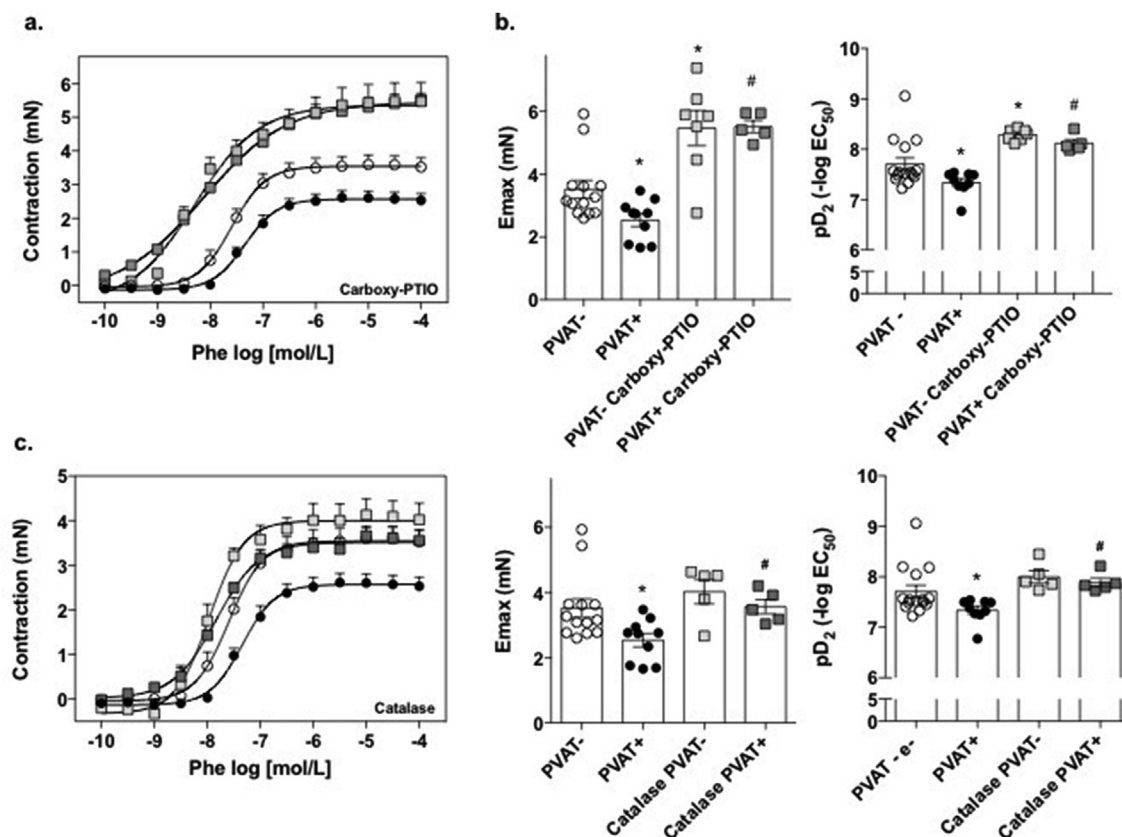


**Fig. 5.** Evaluation of the involvement of NO and H<sub>2</sub>O<sub>2</sub> on the effect of PVAT in vascular contraction induced by Phe. **a-c.** Cumulative concentration-response curves for Phenylephrine, incubated with carboxy-PTIO and catalase, were performed in denuded aortic rings with and without PVAT. **b-d.** Bars represent the mean  $\pm$  SEM of values of Emax and pD<sub>2</sub> of the contraction induced by Phe, in aortic rings incubated with carboxy-PTIO and catalase, obtained in independent preparations. Emax and pD<sub>2</sub> values in denuded aortas, with or without PVAT, and aortas incubated with carboxy-PTIO and catalase. (Carboxy-PTIO PVAT-: n = 7; Carboxy-PTIO PVAT+: n = 5; Catalase PVAT-: n = 5; Catalase PVAT+ n = 5) \*\*#Represents a significant difference (\*p < 0.05 when compared to PVAT-; #p < 0,05 when compared to PVAT+).

significantly reduced in aortas with PVAT (PVAT+) when compared to aortas without PVAT (PVAT-). The Emax and pD<sub>2</sub> values can be visualized in Table 1.

### 3.2. Effect of captopril or Mas and AT<sub>2</sub> receptors antagonists on the contraction induced by Phe in denuded aorta, in the presence or absence of PVAT

As shown in Fig. 1c and d, in aortic rings without endothelium, the incubation with captopril showed that in aortas PVAT-, the presence of this inhibitor did not alter the vascular response when compared with control aortas (PVAT-) that were not incubated with this inhibitor. However, in the aortas PVAT+, the presence of this inhibitor increases both, Emax and pD<sub>2</sub> values, when compared with control aortas (PVAT+) without this inhibitor.

In Fig. 2a and b, the results obtained in the presence of Mas receptor antagonism confirm its involvement on the reduction of Phe-contraction induced by PVAT since the reduction of the contraction that was seen in the PVAT+ control aortas no longer was visualized in the presence of A779. In Fig. 2c and d, in aortic rings with and without PVAT, the AT<sub>2</sub> receptor antagonism reversed only the potency of the contractile response induced by Phe, without changes in Emax values, when compared with control.

### 3.3. Involvement of the PI3K- Akt- pathway in the contraction induced by Phe in denuded aorta in the presence or absence of PVAT

Knowing that the activation of Mas and AT<sub>2</sub> receptors stimulate the

production of NO by NOS activation through PI3k-Akt pathway, the involvement of this pathway was investigated. As demonstrated in Fig. 3a and b, in aortic rings with and without PVAT incubated with inhibitor of PI3k, the reduction of the contraction induced by Phe in the presence of PVAT was totally blocked.

To verify whether NOS is being activated, aortic rings were pre-incubated with the nonselective NOS inhibitor, L-NAME. As shown in Fig. 3c and d, the incubation with L-NAME in aortic rings with and without PVAT totally reverse the contraction when compared to the control response.

After confirming the involvement of NOS in the reduction of vascular contraction induced by Phe in aortic rings with PVAT, we investigated which NOS isoforms could be involved. As shown in Fig. 4a and b, the incubation with L-NNA reversed only pD<sub>2</sub>, without changes in Emax values. In Fig. 4c and d, it was demonstrated that the incubation with 7-Ni reversed only Emax, without changes in pD<sub>2</sub> values when compared to the control group, proving the important involvement of both, nNOS and eNOS, in the anti-contraction effect induced by PVAT.

### 3.4. Involvement of NO and H<sub>2</sub>O<sub>2</sub> in the contraction induced by Phe in denuded aorta in the presence or absence of PVAT

After confirming the important involvement of nNOS and eNOS and knowing that both NO and H<sub>2</sub>O<sub>2</sub> are products of the activation of this enzyme, we investigated whether the reduction of the contraction induced by Phe in the presence of PVAT would be dependent of both. In carboxy-PTIO (Fig. 5a and b) and catalase incubation (Fig. 5c and d)

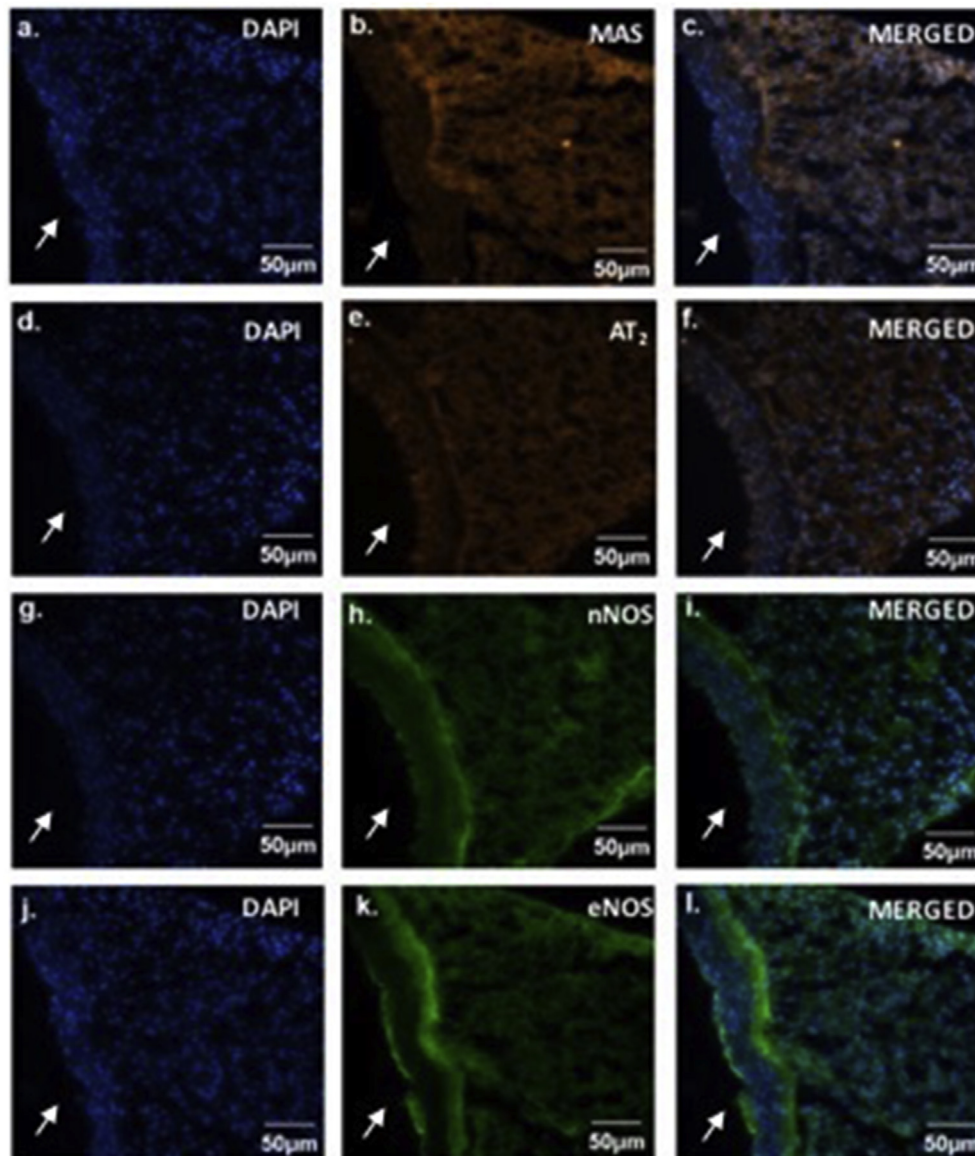
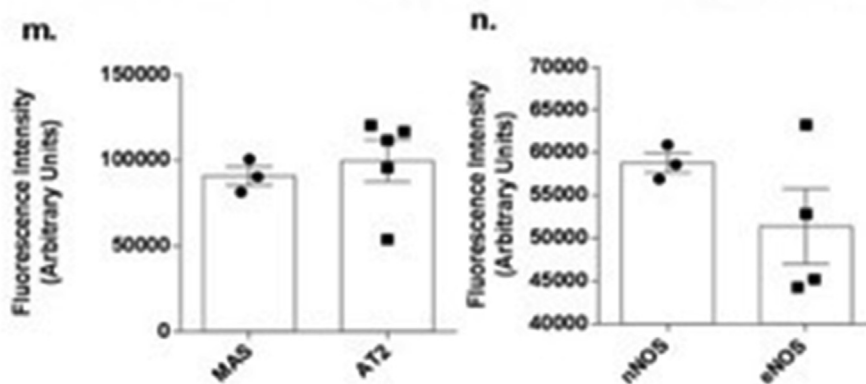


**Fig. 6.** Immunolocalization of Mas and AT<sub>2</sub> receptors, eNOS and nNOS isoform in mice aortas. Representative images of immunofluorescence. **a,d,g and j** - Immunostaining nuclear with DAPI; **b, e, h and k** - Immunostaining Mas and AT<sub>2</sub> receptors, nNOS and eNOS isoform respectively; **c,f,i and l** - Overlap of images Mas and AT<sub>2</sub>, eNOS and nNOS with DAPI; **m and n** - Quantification of the mean fluorescence emitted by binding of the selective secondary antibody to Mas (red fluorescence), AT<sub>2</sub> (red fluorescence), eNOS (green fluorescence) and nNOS (green fluorescence) respectively. (MAS: PVAT+ n = 3; AT<sub>2</sub>: PVAT+ n = 5; nNOS PVAT+ n = 3; eNOS PVAT+ n = 4). Scale bar equals 50 μm. White arrows indicate vessel lumen.



showed that the reduction of the Phe vascular contraction in the presence of PVAT is NO and H<sub>2</sub>O<sub>2</sub> dependent.

### 3.5. Immunolocalization

After confirming the involvement of Mas and AT<sub>2</sub> receptors and activation of the eNOS and nNOS enzymes in the reduction of the

contraction induced by Phe in denuded aorta in the presence of PVAT, we investigated the location of these receptors and enzymes in aortic rings.

In Fig. 6 we demonstrate where Mas (6a to 6c) and AT<sub>2</sub> (6d to 6f) receptors would be located in aortic rings. Our results demonstrated that Mas receptors are widely located in both PVAT and tunica intima indicated by intense fluorescence in red, whereas the AT<sub>2</sub> receptors

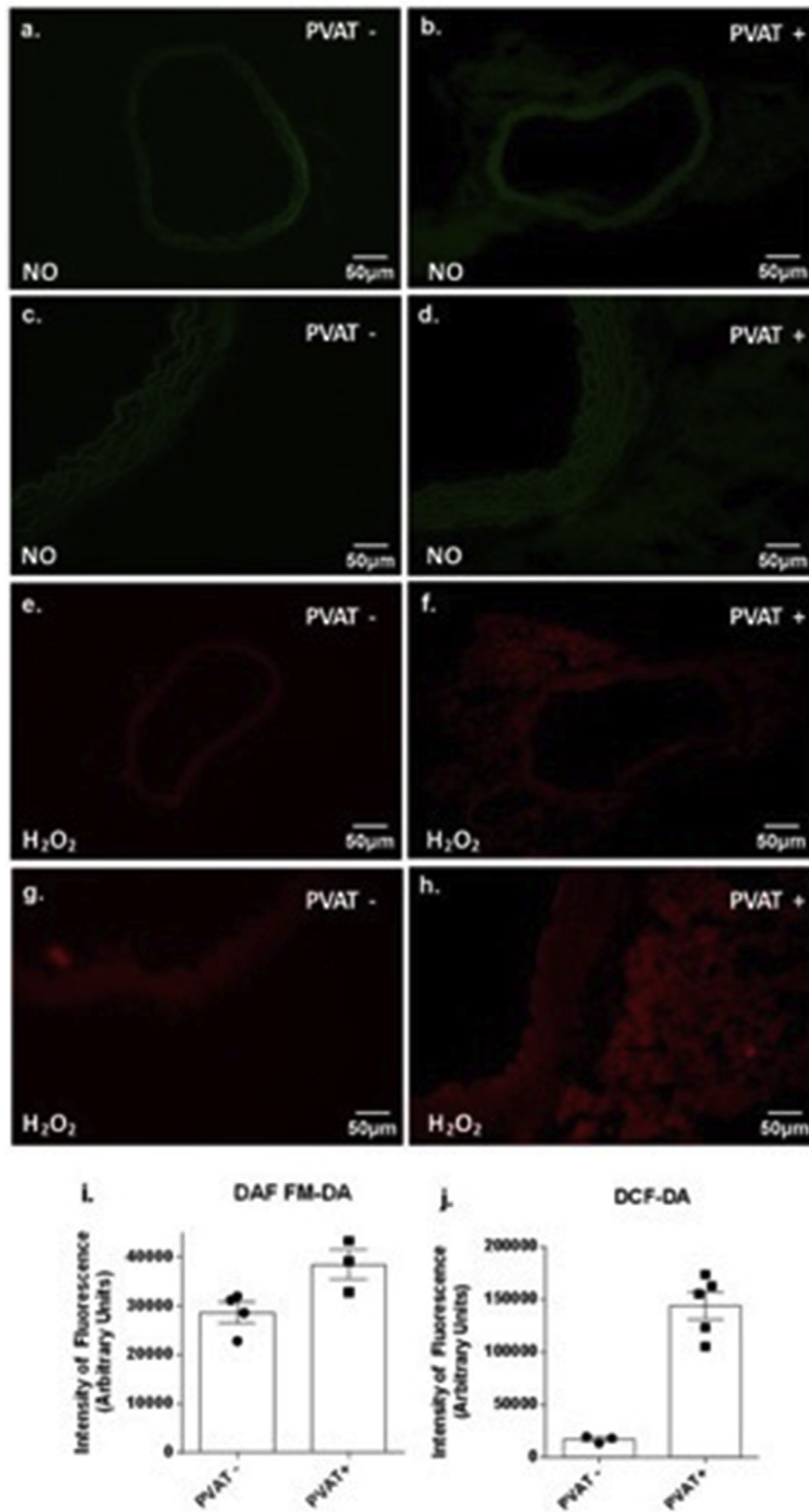


**Fig. 7.** Fluorescence emitted by the NO selective probe (DAF-FM DA) and H<sub>2</sub>O<sub>2</sub> selective probe (DCF-DA), showing the location of NO and H<sub>2</sub>O<sub>2</sub> in aortas with and without PVAT. DAF-FM DA; fluorescence indicates nitric oxide presence, and the DCF-DA indicates hydrogen peroxide presence. Representative images of aortic rings with and without PVAT. **a-e** - Aortas without PVAT (10×); **b-f** - Aortas with PVAT (10×); **c-g** - Aortas without PVAT (40×); **d-h** - Aortas with PVAT (40×). DAF-FM DA (green fluorescence) and DCF-DA (red fluorescence) respectively; **i** and **j** - Bars with distribution represent a quantification of the mean fluorescence emitted by binding of the selective probe to NO and H<sub>2</sub>O<sub>2</sub> respectively. (DAF-FM DA: PVAT- n = 4; PVAT+ n = 3; DCF-DA: PVAT- n = 3; PVAT + n = 5). \*Represents a significant difference (\*p < 0.05 when compared to PVAT-). Scale bar equals 50 μm.

showed a fluorescence in red in some regions of PVAT. Therefore, these results demonstrated the presence of Mas and AT<sub>2</sub> receptors in PVAT.

In the same figure, our results confirmed the presence of both nNOS (6g to 6i) and eNOS (6j to 6l) isoforms in mice aortas. nNOS isoform is distributed throughout the PVAT, which is confirmed by intense fluorescence in green in this tissue. eNOS is found in the tunica intima and in some points of PVAT demonstrated by the intense green

fluorescence in the endothelial layer and a low fluorescence in PVAT.

### 3.6. NO and H<sub>2</sub>O<sub>2</sub> detection

As shown in Fig. 7, our results demonstrated that the fluorescence intensity for NO (7a to 7d and 7j) and H<sub>2</sub>O<sub>2</sub> (7e to 7h and 7j) are increased in aortic rings with PVAT when compared to aortic rings

without PVAT.

#### 4. Discussion

The PVAT is currently characterized as a biologically active tissue and vascular tone modulator [4,34]. The ability of this tissue to reduce the vasoconstriction response is well known. Soltis & Cassis (1991) demonstrated that the vascular contraction induced by noradrenaline in rat aortas is attenuated in the presence of PVAT [35]. In the same way, Gao et al. (2005) verified that the transfer of nutrient solution from in humans thoracic aortas with PVAT to aortas without PVAT reduced the contractile response induced by Phe [36]. Although the PVAT regulatory effect on vascular tone has been shown, a better understanding of the role of this tissue is necessary.

Therefore, knowing that PVAT acts reducing the maximum effect and potency of the vasoconstrictor response in both rat and human aortas, could this same response profile be found in mice aortas?

Our group has proven that PVAT has a negative regulatory activity in mice aortas, reducing the maximum effect and potency of vasoconstriction induced by Phe. This result corroborates with Boydens et al. (2015) that demonstrated, in Swiss mice aortas, a reduction of the contractile response induced in the presence of PVAT [37]. However, our results differ from these mentioned once we verified the effect of PVAT, in Balb/c mice aortas, just in the absence of endothelium.

This is in accordance with the results presented by Gao et al. (2007) which demonstrated that the effect of PVAT can occur through two different pathways, one dependent on the endothelium and another endothelium-independent, in which the latter involves the increase of H<sub>2</sub>O<sub>2</sub> production and activation of guanylate cyclase (GCs) [10].

In the literature, the PVAT is characterized as a high plasticity tissue releasing different substances depending on the vessels and/or the situation in which this tissue is submitted [13].

Dubrovskaja et al. (2004), verified that the reduction of vasoconstriction response can be induced by different factors, such as the PVRF, not yet identified [9]. Lee et al. (2009) demonstrated that Ang 1–7 is one of the factors released by PVAT in Wistar aorta [14]. In 2011, this same group proved the involvement of Mas receptors activation in reducing contractile response induced by PVAT [14,18]. Considering these findings, we started the investigation of the involvement of renin-angiotensin system (RAS) in the effect triggered by PVAT in mice aortas.

Incubation of the aortas with captopril confirms the crucial involvement of the vasodilators factors derived from ACE in the effect of PVAT. These results corroborate the data published that demonstrates the expression of renin-angiotensin system components such as angiotensinogen and ACE 2 in adipose tissue and perivascular adipose tissue [16,38,39]. Thus, our results confirming the involvement of RAS in the PVAT effect.

The factors produced by ACE can induce vascular relaxation by activation of Mas and AT<sub>2</sub> receptors [40,41]. With vascular reactivity experiments, results proved the involvement of both receptors in the effect of PVAT on the vascular tone and we observed, for the first time in the literature, that these receptors are located in PVAT.

Sampaio et al. (2007), demonstrated that Mas activation in endothelium cells induces NO production by NOS via PI3k/Akt [19]. Our results demonstrated the involvement of PI3k, eNOS and nNOS in the anti-contractile response induced by PVAT. In addition, we confirm the presence of both NOS isoforms, eNOS and nNOS, in PVAT.

According to Capettini et al. (2008) the nNOS isoform produces not only NO but also H<sub>2</sub>O<sub>2</sub>, both vasodilators factors [42–44]. Hayabuchi et al. (1998) demonstrated that H<sub>2</sub>O<sub>2</sub> induces the relaxation of conductance arteries by guanylate cyclase activation and potassium channel calcium dependent open [42,45]. This present study confirm the presence of NO and H<sub>2</sub>O<sub>2</sub> in PVAT, corroborating with the negative modulatory effect of PVAT on the vascular tone.

#### 5. Conclusion

In summary, the present study shows that PVAT reduces the contractile response induced by phenylephrine; however, this effect is only verified in the absence of vascular endothelium. In addition, the control of vascular tone triggered by PVAT mainly involves Mas receptor activation with consequent PI3k/Akt pathway and nNOS activation in this process. The involvement of nNOS leads to an increase in the production of NO and H<sub>2</sub>O<sub>2</sub> to be the main vasodilators responsible for the anti-contractile effect of PVAT. It should be noted that PVAT effect also involves activation of AT<sub>2</sub> receptors and the eNOS isoform; however, in a less important way.

It is important to highlight that this control pathway of the vascular tone induced by PVAT is unprecedented in the literature, as well as the results that show the presence of Mas and AT<sub>2</sub> receptors, as well as, nNOS and eNOS enzymes in the PVAT.

#### Acknowledgements

I would like to thank all the people involved in this work mainly Prof. Dr<sup>o</sup> Helton José dos Reis team for availability and attention in fluorescence microscopy analysis and Pedro Henrique Ferreira Sucupira for support and dedication for formatting this paper.

#### Appendix A. Supplementary data

Supplementary data to this article can be found online at <https://doi.org/10.1016/j.niox.2018.12.011>.

#### Funding

This work was supported by grants from Fundação de Amparo à Pesquisa do Estado de Minas Gerais [grant numbers CBB-APQ 0202014] and Coordenação de Aperfeiçoamento de Pessoal de Nível Superior [grant numbers 1424569].

#### Conflict of interest

The authors report no commercial or proprietary interest in any product or concept discussed in this article.

#### References

- [1] C. Barandier, J.P. Montani, Z. Yang, Mature adipocytes and perivascular adipose tissue stimulate vascular smooth muscle cell proliferation: effects of aging and obesity, *Am. J. Physiol. Heart Circ. Physiol.* 289 (2005) H1807–H1813, <https://doi.org/10.1152/ajpheart.01259.2004>.
- [2] S. Rajshaker, D. Manka, A.L. Blomkalns, T.K. Chatterjee, L.L. Stoll, N.L. Weintraub, Crosstalk between perivascular adipose tissue and blood vessels, *Curr. Opin. Pharmacol.* 10 (2010) 191–196, <https://doi.org/10.1016/j.coph.2009.11.005>.
- [3] S. Verlohren, G. Dubrovskaja, S.Y. Tsang, K. Essin, F.C. Luft, Y. Huang, M. Gollasch, Visceral periaortic adipose tissue regulates arterial tone of mesenteric arteries, *Hypertension* 44 (2004) 271–276, <https://doi.org/10.1161/01.HYP.0000140058.28994.ec>.
- [4] Y.J. Gao, Dual modulation of vascular function by perivascular adipose tissue and its potential correlation with adiposity/lipoatrophy-related vascular dysfunction, *Curr. Pharmaceut. Des.* 13 (2007) 2185–2192 <http://www.ncbi.nlm.nih.gov/pubmed/17627551>.
- [5] E.E. Kershaw, J.S. Flier, Adipose tissue as an endocrine organ, *J. Clin. Endocrinol. Metab.* 89 (2004) 2548–2556, <https://doi.org/10.1210/jc.2004-0395>.
- [6] S. Cinti, The adipose organ, *Prostaglandins Leukot. Essent. Fatty Acids* 73 (2005) 9–15, <https://doi.org/10.1016/j.plefa.2005.04.010>.
- [7] H. Tilg, A.R. Moschen, Adipocytokines: mediators linking adipose tissue, inflammation and immunity, *Nat. Rev. Immunol.* 6 (2006) 772–783, <https://doi.org/10.1038/nri1937>.
- [8] A. Frontini, S. Cinti, Distribution and development of brown adipocytes in the murine and human adipose organ, *Cell Metab.* 11 (2010) 253–256, <https://doi.org/10.1016/j.cmet.2010.03.004>.
- [9] G. Dubrovskaja, S. Verlohren, F.C. Luft, M. Gollasch, Mechanisms of ADRF release from rat aortic adventitial adipose tissue, *Am. J. Physiol. Heart Circ. Physiol.* 286 (2004) H1107–H1113, <https://doi.org/10.1152/ajpheart.00656.2003>.
- [10] Y.-J. Gao, C. Lu, L.-Y. Su, A.M. Sharma, R.M.K.W. Lee, Modulation of vascular

- function by perivascular adipose tissue: the role of endothelium and hydrogen peroxide, *Br. J. Pharmacol.* 151 (2007) 323–331, <https://doi.org/10.1038/sj.bjp.0707228>.
- [11] M. Lohn, G. Dubrovskaja, B. Lauterbach, F.C. Luft, M. Gollasch, A.M. Sharma, Periadventitial fat releases a vascular relaxing factor, *FASEB J.* 16 (2002) 1057–1063, <https://doi.org/10.1096/fj.02-0024com>.
- [12] G. Fesus, G. Dubrovskaja, K. Gorzelnik, R. Kluge, Y. Huang, F.C. Luft, M. Gollasch, Adiponectin is a novel humoral vasodilator, *Cardiovasc. Res.* 75 (2007) 719–727, <https://doi.org/10.1016/j.cardiores.2007.05.025>.
- [13] B. Galvez-Prieto, B. Somoza, M. Gil-Ortega, C.F. Garcia-Prieto, A.I. de las Heras, M.C. Gonzalez, S. Arribas, I. Aranguez, J. Bolbrinker, R. Kreuz, M. Ruiz-Gayo, M.S. Fernandez-Alfonso, Anticontractile effect of perivascular adipose tissue and leptin are reduced in hypertension, *Front. Pharmacol.* 3 (2012) 103, <https://doi.org/10.3389/fphar.2012.00103>.
- [14] R.M. Lee, C. Lu, L.Y. Su, Y.J. Gao, Endothelium-dependent relaxation factor released by perivascular adipose tissue, *J. Hypertens.* 27 (2009) 782–790, <https://doi.org/10.1097/HJH.0b013e328324ed86>.
- [15] M. Gil-Ortega, P. Stucchi, R. Guzman-Ruiz, V. Cano, S. Arribas, M.C. Gonzalez, M. Ruiz-Gayo, M.S. Fernandez-Alfonso, B. Somoza, Adaptive nitric oxide overproduction in perivascular adipose tissue during early diet-induced obesity, *Endocrinology* 151 (2010) 3299–3306, <https://doi.org/10.1210/en.2009-1464>.
- [16] B. Galvez-Prieto, J. Bolbrinker, P. Stucchi, A.I. de las Heras, B. Merino, S. Arribas, M. Ruiz-Gayo, M. Huber, M. Wehland, R. Kreuz, M.S. Fernandez-Alfonso, Comparative expression analysis of the renin-angiotensin system components between white and brown perivascular adipose tissue, *J. Endocrinol.* 197 (2008) 55–64, <https://doi.org/10.1677/JOE-07-0284>.
- [17] Y.J. Gao, K. Takemori, L.Y. Su, W.S. An, C. Lu, A.M. Sharma, R.M. Lee, Perivascular adipose tissue promotes vasoconstriction: the role of superoxide anion, *Cardiovasc. Res.* 71 (2006) 363–373, <https://doi.org/10.1016/j.cardiores.2006.03.013>.
- [18] R.M. Lee, M. Bader, N. Alenina, R.A. Santos, Y.J. Gao, C. Lu, Mas receptors in modulating relaxation induced by perivascular adipose tissue, *Life Sci.* 89 (2011) 467–472, <https://doi.org/10.1016/j.lfs.2011.07.016>.
- [19] W.O. Sampaio, R.A.S. Dos Santos, R. Faria-Silva, L.T. Da Mata Machado, E.L. Schiffrin, R.M. Touyz, Angiotensin-(1-7) through receptor Mas mediates endothelial nitric oxide synthase activation via Akt-dependent pathways, *Hypertension* 49 (2007) 185–192, <https://doi.org/10.1161/01.HYP.0000251865.35728.2f>.
- [20] M.C. Diniz, V.C. Olivon, L.D. Tavares, J.A. Simplicio, N.A. Gonzaga, D.G. de Souza, L.M. Bendhack, C.R. Tirapelli, D. Bonaventura, Mechanisms underlying sodium nitroprusside-induced tolerance in the mouse aorta: Role of ROS and cyclooxygenase-derived prostanoids, *Life Sci.* 176 (2017) 26–34, <https://doi.org/10.1016/j.lfs.2017.03.016>.
- [21] C. Lu, L.Y. Su, R.M.K.W. Lee, Y.J. Gao, Alterations in perivascular adipose tissue structure and function in hypertension, *Eur. J. Pharmacol.* 656 (2011) 68–73, <https://doi.org/10.1016/j.ejphar.2011.01.023>.
- [22] A.M. Van Der Graaf, M.J. Wiegman, T. Plösch, G.G. Zeeman, A. Van Buiten, R.H. Henning, H. Buikema, M.M. Faas, Endothelium-dependent relaxation and angiotensin II sensitivity in experimental preeclampsia, *PLoS One* 8 (2013), <https://doi.org/10.1371/journal.pone.0079884>.
- [23] O. Moreno Loaiza, A. Paz Aliaga, Efecto vasodilatador mediado por óxido nítrico del extracto hidroalcohólico de zea mays L (Maiz morado) en anillo aórtico de rata, *Rev. Peru. Med. Exp. Salud Pública* 27 (2010) 527–531.
- [24] R. Jimenez, M. Sanchez, M.J. Zarzuelo, M. Romero, A.M. Quintela, R. Lopez-Sepulveda, P. Galindo, M. Gomez-Guzman, J.M. Haro, A. Zarzuelo, F. Perez-Vizcaino, J. Duarte, Endothelium-dependent vasodilator effects of peroxisome proliferator-activated receptor agonists via the phosphatidylinositol-3 kinase-akt pathway, *J. Pharmacol. Exp. Therapeut.* 332 (2010) 554–561, <https://doi.org/10.1124/jpet.109.159806>.
- [25] A.V. Araújo, C.Z. Ferezin, A. de C. Pereira, G.J. Rodrigues, M.D. Grando, D. Bonaventura, L.M. Bendhack, Augmented nitric oxide production and up-regulation of endothelial nitric oxide synthase during cecal ligation and perforation, *Nitric Oxide* 27 (2012) 59–66, <https://doi.org/10.1016/j.niox.2012.04.005>.
- [26] A. Yogi, G.E. Callera, U.V. Hipólito, C.R. Silva, R.M. Touyz, C.R. Tirapelli, Ethanol-induced vasoconstriction is mediated via redox-sensitive cyclo-oxygenase-dependent mechanisms, *Clin. Sci. (Lond.)* 118 (2010) 657–668, <https://doi.org/10.1042/CS20090352>.
- [27] J.M. McCord, I. Fridovich, Superoxide dismutase, *J. Biol. Chem.* 244 (1969) 6049–6055 <http://www.jbc.org/content/244/22/6049.abstract%5Cnhttp://www.jbc.org/content/244/22/6049.full.pdf%5Cnhttp://www.jbc.org/content/244/22/6049.full.pdf+html?frame=sidebar>.
- [28] J.C. Wanstall, T.K. Jeffery, A. Gambino, F. Lovren, C.R. Triggle, Vascular smooth muscle relaxation mediated by nitric oxide donors: a comparison with acetylcholine, nitric oxide and nitroxyl ion, *Br. J. Pharmacol.* (2001), <https://doi.org/10.1038/sj.bjp.0704269>.
- [29] A.P. Davel, J.A. Victorio, M.A. Delbin, L.E. Fukuda, L.V. Rossoni, Enhanced endothelium-dependent relaxation of rat pulmonary artery following ??-adrenergic overstimulation: involvement of the NO/cGMP/VASP pathway, *Life Sci.* 125 (2015) 49–56, <https://doi.org/10.1016/j.lfs.2015.01.018>.
- [30] J.A. Victorio, M.T. Fontes, L.V. Rossoni, A.P. Davel, Different anti-contraction function and nitric oxide production of thoracic and abdominal perivascular adipose tissues, *Front. Physiol.* 7 (2016), <https://doi.org/10.3389/fphys.2016.00295>.
- [31] A.P. Davel, J.A. Victorio, M.A. Delbin, L.E. Fukuda, L.V. Rossoni, Enhanced endothelium-dependent relaxation of rat pulmonary artery following ??-adrenergic overstimulation: involvement of the NO/cGMP/VASP pathway, *Life Sci.* 125 (2015) 49–56, <https://doi.org/10.1016/j.lfs.2015.01.018>.
- [32] J.M. Navia-Pelaez, G.P. Campos-Mota, J.C. Araujo de Souza, E.C. Aguiar, N. Stergiopoulos, J.I. Alvarez-Leite, L.S.A. Capellini, nNOS uncoupling by oxidized LDL: implications in atherosclerosis, *Free Radic. Biol. Med.* 113 (2017) 335–346, <https://doi.org/10.1016/j.freeradbiomed.2017.09.018>.
- [33] M.J. Curtis, R.A. Bond, D. Spina, A. Ahluwalia, S.P.A. Alexander, M.A. Giembycz, A. Gilchrist, D. Hoyer, P.A. Insel, A.A. Izzo, A.J. Lawrence, D.J. Macewan, L.D.F. Moon, S. Wonnacott, A.H. Weston, J.C. McGrath, Experimental design and analysis and their reporting: new guidance for publication in *BJP*, *Br. J. Pharmacol.* 172 (2015) 3461–3471, <https://doi.org/10.1111/bph.12856>.
- [34] M. Gollasch, G. Dubrovskaja, Paracrine role for periadventitial adipose tissue in the regulation of arterial tone, *Trends Pharmacol. Sci.* 25 (2004) 647–653, <https://doi.org/10.1016/j.tips.2004.10.005>.
- [35] E.E. Soltis, L.A. Cassis, Influence of perivascular adipose tissue on rat aortic smooth muscle responsiveness, *Clin. Exp. Hypertens.* 13 (1991) 277–296 <http://www.ncbi.nlm.nih.gov/pubmed/2065467>.
- [36] Y.J. Gao, A.C. Holloway, Z.H. Zeng, G.E. Lim, J.J. Petrik, W.G. Foster, R.M. Lee, Prenatal exposure to nicotine causes postnatal obesity and altered perivascular adipose tissue function, *Obes. Res.* 13 (2005) 687–692, <https://doi.org/10.1038/oby.2005.77>.
- [37] C. Boydens, B. Pauwels, J. Van de Voorde, Effect of resveratrol and orchidectomy on the vasorelaxing influence of perivascular adipose tissue, *Heart Ves.* (2015), <https://doi.org/10.1007/s00380-015-0664-2>.
- [38] J. Aubert, C. Darimont, I. Safonova, G. Ailhaud, R. Negrel, Regulation by glucocorticoids of angiotensinogen gene expression and secretion in adipose cells, *Biochem. J.* 328 (Pt 2) (1997) 701–706 <http://www.pubmedcentral.nih.gov/articlerender.fcgi?artid=1218974&tool=pmcentrez&rendertype=abstract>.
- [39] C. Karlsson, K. Lindell, M. Ottosson, L. Sjöström, B. Carlsson, L.M. Carlsson, Human adipose tissue expresses angiotensinogen and enzymes required for its conversion to angiotensin II, *J. Clin. Endocrinol. Metab.* 83 (1998) 3925–3929, <https://doi.org/10.1210/jcem.83.11.5276>.
- [40] T. Unger, The role of the renin-angiotensin system in the development of cardiovascular disease, *Am. J. Cardiol.* 89 (2002) 3A–9A discussion 10A <http://www.ncbi.nlm.nih.gov/pubmed/11835903>.
- [41] A. Nguyen Dinh Cat, R.M. Touyz, A new look at the renin-angiotensin system—focusing on the vascular system, *Peptides* 32 (2011) 2141–2150, <https://doi.org/10.1016/j.peptides.2011.09.010>.
- [42] L.S. a. Capellini, S.F. Cortes, M. a. Gomes, G. a. B. Silva, J.L. Pesquero, M.J. Lopes, M.M. Teixeira, V.S. Lemos, Neuronal nitric oxide synthase-derived hydrogen peroxide is a major endothelium-dependent relaxing factor, *Am. J. Physiol. Heart Circ. Physiol.* 295 (2008) H2503–H2511, <https://doi.org/10.1152/ajpheart.00731.2008>.
- [43] G.C. Silva, J.F. Silva, T.F. Diniz, V.S. Lemos, S.F. Cortes, Endothelial dysfunction in DOCA-salt-hypertensive mice: role of neuronal nitric oxide synthase-derived hydrogen peroxide, *Clin. Sci.* (2016), <https://doi.org/10.1042/CS20160062>.
- [44] P.W. Endlich, R.D. Aires, R.L. Gonçalves, E.D. Costa, J. de Paula Arantes Ângelo, L.F. Alves, R.F. da Silva, B.A. Rezende, S.F. Cortes, V.S. Lemos, Neuronal nitric oxide synthase-derived hydrogen peroxide effect in grafts used in human coronary bypass surgery, *Clin. Sci.* (2017), <https://doi.org/10.1042/CS20160642>.
- [45] Y. Hayabuchi, Y. Nakaya, S. Matsuoka, Y. Kuroda, Hydrogen peroxide-induced vascular relaxation in porcine coronary arteries is mediated by Ca<sup>2+</sup>-activated K<sup>+</sup> channels, *Heart Ves.* 13 (1998) 9–17 <http://www.ncbi.nlm.nih.gov/pubmed/9923560>.